Scanning Thermopower Microscopy of Guanine Monolayers

J. C. Poler,* R. M. Zimmermann, and Edward C. Cox

Department of Molecular Biology, Princeton University, Princeton, New Jersey 08544

Received November 29, 1994. In Final Form: February 17, 1995[⊗]

Thermally deposited monolayers of the DNA base guanine have been studied by scanning tunneling microscopy (STM) and a novel scanning thermopower microscope (STPM). The STPM signal provides a distinct representation of the monolayer lattice not present in the STM signal. The intensity of the thermopower contrast is dependent on the temperature gradient at the tunnel junction. Surface roughness and topographical variations of the underlying substrate are not convoluted with the signal due to the feed-forward acquisition method of this technique. A plausible interpretation of the STPM signal and images is proposed, and the prospects for single molecule differentiation and spectroscopy are discussed.

Introduction

The scanning tunneling microscope (STM)[1] and atomic force microscope (AFM)[2] are standard tools used to investigate surfaces and monolayers adsorbed to surfaces.[3-9] Most monolayers energetically favor a two-dimensional (2D) lattice structure, and hence the order within these lattices is often unambiguous, especially with AFM. However, STM images are typically a convolution of the molecular lattice and the underlying substrate, which can make single molecule identification difficult. In particular, the asignment of position and orientation of two similar molecules in the same lattice can be problematic. Although Hallmark *et al.*[3] found it possible to distinguish naphthalene from azulene on Pt by STM, even with their high resolution topographs, tedious image analysis was required to make the molecular assignments. This problem is exacerbated when the molecular image is also convoluted by electronic coupling to the substrate, as is often the case for studies on highly oriented pyrolytic graphite (HOPG).[10] Moreover, when the molecule is not planar (e.g., polymer chains with pendant side groups), or not oriented parallel to the substrate (e.g., purines on Au(111)[11] and self-assembled monolayers of alkanethiols[12]), molecular discrimination by topography alone is often impossible.

Many of these difficulties can in principle be overcome by methods based on single molecule spectroscopy. Recent advances in this approach include near field scanning optical microscopy, where it has proven possible to observe the fluorescent emission of individual dye molecules,[13] atomic resolution local density of states (LDOS) spectra of individual Fe atoms on Cu(111),[14] and sub-nanometer resolution of the vibrational spectroscopy of sorbic acid on HOPG.[15] Other promising results include an electron spin resonance STM study of defect states in SiO_2[16] and an AFM-based magnetic resonance force analysis of diphenylpicrylhydrazil adsorbates.[17]

The work on which we report here, directed toward the goal of single molecule spectroscopy, is an application of a result obtained by Williams and Wickramasinghe,[18] who imaged MoS_2 and HOPG surfaces by measuring the lateral variations of the thermopower signal (Q) across a tip–sample temperature gradient. We call this method scanning thermopower microscopy (STPM). Because the chemical potential at a surface is dependent on the local electronic nature of the unsatisfied bonding at the crystal face,[19] it will be affected by the presence of molecular adsorbates. We find this to be the case, and report here on our STPM investigations of Guanine (G) monolayers adsorbed to HOPG. The STPM images provide additional information about the monolayers that STM images alone do not. The thermopower signal is not strongly convoluted with the topography of the sample and substrate. This is an important feature, since it enables molecular identification regardless of molecular internal structure or orientation.

Experimental Section

To acquire the STPM images we modified a commercially available STM (Topometrix). Figure 1 illustrates the additional electronics employed for simultaneous measurement of topography and thermopower. The thermopower signal is the voltage measured between the tip and the heated sample, similar to the work of Williams and Wickramasinghe.[18] To reduce noise in the electronics, we shielded input lines and used a battery-driven power supply. The input line to the tip was in a guarded configuration to reduce cable capacitance. A differential amplifier, with high input impedance and ultralow input bias current buffer amplifiers (Burr Brown), was used to minimize leakage currents to <100 fA. The sample temperature was controlled by a thin film substrate heater (Minco), which was powered by a low noise constant current source (Kepco) followed by a low-pass

[⊗] Abstract published in *Advance ACS Abstracts,* June 1, 1995.

(1) Binning, G.; Rohrer, H.; Gerber, C.; Weibel, E. *Phys. Rev. Lett.* **1982**, *49*, 57.
(2) Binning, G.; Quate, C. F.; Gerber, C. *Phys. Rev. Lett.* **1986**, *56*, 930.
(3) Hallmark, V. M.; Chiang, S.; Meinhardt, K.-P.; K. Hafner *Phys. Rev. Lett.* **1993**, *70*, 3740–3.
(4) Frommer, J. *Angew. Chem., Int. Ed. Engl.* **1992**, *31*, 1298–1328.
(5) Burrows, P. E.; Zhang, Y.; Haskal, E. I.; Forrest, S. R. *Appl. Phys. Lett.* **1992**, *61*, 2417–9.
(6) Bucher, J.-P.; Roeder, H.; Kern, K. *Surf. Sci.* **1993**, *289*, 370–80.
(7) Lippel, P. H.; Wilson, R. J.; Miller, M. D.; Wöll, C.; Chiang, S. *Phys. Rev. Lett.* **1989**, *62*, 171–4.
(8) Madsen, L. L.; Jørgensen, J. F.; Carneiro, K.; Jørgensen, M.; Garnaes, J. *Synth. Met.* **1993**, *55–57*, 335–40.
(9) Wang, P.; Shamsuzzoha, M.; Lee, W.-J.; Wu, X.-L.; Metzger, R. M. *Synth. Met.* **1993**, *55–57*, 3104–9.
(10) Heckl, W. M.; Smith, D. P. E.; Binning, G.; Klagges, H.; Hänsch, T. W.; Maddocks, J. *Proc. Natl. Acad. Sci.* **1991**, *88*, 8003–5.
(11) Tao, N. J.; DeRose, J. A.; Lindsay, S. M. *J. Phys. Chem.* **1993**, *97*, 910–19.
(12) Poirier, G. E.; Tarlov, M. J. *Langmuir* **1994**, *10*, 2853–2856.
(13) Betzig, E.; Chichester, R. J. *Science* **1993**, *262*, 1422–5.
(14) Crommie, M. F.; Lutz, C. P.; Eigler, D. M. *Phys. Rev. B* **1993**, *48*, 2851–4.
(15) Smith, D. P. E.; Kirk, M. D.; Quate, C. F. *J. Chem. Phys.* **1987**, *86*, 6034–8.
(16) Manassen, Y.; Ter-Ovanesyan, E.; Shachal, D.; Richter, S. *Phys. Rev. B* **1993**, *48*, 4887–90.
(17) Züger, O.; Rugar, D. *Appl. Phys. Lett.* **1993**, *63*, 2496–8.
(18) Williams, C. C.; Wickramasinghe, H. K. *Nature* **1990**, *344*, 317–9.
(19) Sze, S. M. *Physics of Semiconductor Devices,* 2 ed.; John Wiley & Sons: New York, 1981; p 248.

0743-7463/95/2411-2689$09.00/0

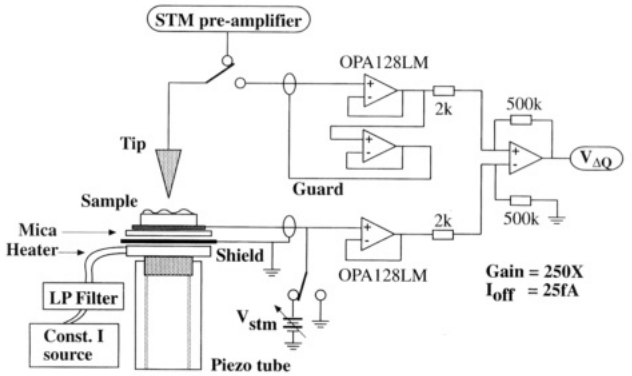

Figure 1. 1. Scanning thermopower microscope. A high input impedance, ultralow input bias current, differential amplifier measures the thermopower voltage between the tip and the sample. The sample is heated by a thin film heater and rastered by the piezo-tube scanner.

filter ($f_c \sim 1$ Hz). A grounded metal shield between sample and the piezo-tube eliminated capacitive pickup on the thermopower signal.

A digital signal processor controlled the scanning and feedback mechanisms. The processor's algorithm was modified to enable two consecutive scans over the same line. The first line scan measured the tunneling current topography using a feedback loop. The resulting profile was stored, and the scanner was repositioned at the beginning of the line. Simultaneously, the feedback loop was opened, the bias on the sample was switched to ground and the differential amplifier was switched into the circuit. Because of an initial switching transient, the thermopower electronics required approximately 50 ms to stabilize. The same line was then rescanned and the thermopower voltage measured. The previously stored topographic data were used to keep the tip−sample gap impedance constant (i.e., feed-forward mode) during the second scan. Sample drift and topography errors were minimized by adjusting the scanning parameters. A test mode that measured the tunneling current, instead of the thermopower, during the second feed-forward scan determined the accuracy of the algorithm. Since there was no change in tunneling current during the second scan (i.e., no contrast in the STM image), we conclude that the topography was reproduced by the piezo scanner. Both the STM and STPM images were displayed simultaneously for comparison.

Two fine-gauge thermocouples (K-type, 12.7 μm diameter, Omega) measured the temperature difference between the heated sample and the tip. The first thermocouple was mounted to the tip with silver epoxy. A microscope was used to place the junction as close as possible to the tip end (~750 μm). The second thermocouple was placed on the HOPG surface and embedded in graphite paint. The tip was then centered above the second thermocouple and brought closer to it with the stepper motor. We stopped the approach as soon as the tip contacted the surface, indicated by current flow. This position approximated the tip−surface distance during scanning in feedback. Temperature measurements of the tip and the sample were simultaneous. Finally, the tip was backed away from the surface to determine temperature changes on the tip and sample due to the close thermal contact. The temperature difference as a function of current through the sample heater was used for calibration. The piezo-tube sensitivity was also calibrated at different temperatures. This calibration was done by measuring the lattice constant of HOPG under varying rotation angles of the sample. The variation of the piezo sensitivity (Å/V) at higher substrate temperatures, ~70 °C, was 20% lower than at room temperature. Images were corrected accordingly.

Single crystalline Au(111) (Alfa AESAR) was cleaned in a solution of $H_2O/NH_4OH/H_2O_2$ (4/1/1) at 70 °C for 1 h. The surface was then flame annealed for 5 min with a propane−O_2 torch. The Au was immediately quenched in an alkanethiol solution.[20]

Guanine monolayers were deposited from saturated solutions of guanine (Sigma) in distilled, deionized and micropore-filtered H_2O. From UV absorption (a_m(252 nm) = 13.7 × 10^3), we determined the saturation concentration to be 36 μM. Freshly cleaved HOPG was heated in an Al block held at 85 °C. After a several minute warm up period, 10 μL of the guanine solution was applied to the HOPG.[21] The water evaporated to dryness in ~2 min. As the water volume decreased, the perimeter of the drop started to contract. After 10−50% contraction, the area of the drop stabilized. Further reduction of the volume resulted in a flattening of the drop. Finally, the drop became so thin that the remaining solvent snapped to the outer edge of the drop due to surface tension. This procedure almost always deposits a guanine layer. The sample was cooled in air.[22] STM images of stable and ordered monolayers are reproducible and obtained approximately 10% of the time. In almost all depositions, there was some type of structure not associated with the HOPG substrate. Negative control studies with depositions of pure distilled and deionized water never (~5 depositions and hundreds of scanned images) revealed any of the structures described below.

Results and Discussion

Topographic Independence of the STPM Signal. To measure the thermopower open circuit potential, it was important that the leakage current in the electronics be minimized. Any current between the tip and the sample results in an ohmic potential drop, which varies with gap impedance changes. The result can be a topography-dependent signal, which adds to the thermopower signal. For example, with an input bias current of 1 pA (standard amplifiers, e.g., LF411), and a 1-GΩ gap impedance, distance variations of only 0.1 Å result in 116-μV signal variations. This value is comparable to typical ΔQ variations on substrates or monolayers (between 200 and 500 μV, as discussed below). In our electronics we reduced the leakage currents to less than 100 fA. Scanning at low gap impedance (10 MΩ) with this design leads to ohmic potentials < 2 μV due to height variations of 0.5 Å. This is more than an order of magnitude below typically measured ΔQ values. In all our experiments we measured the ΔQ signal in constant height feed-forward mode. In this mode STM experiments showed that the feedback loop was able to follow and reproduce the topography to within 0.1 Å accuracy normal to the surface. Therefore this voltage can be made insensitive to corrugation heights even at higher gap impedance, where leakage current induced ohmic potentials become significant. This permits the use of a higher gap impedance range, which reduces tip−sample mechanical interactions.

STM and STPM studies of Au(111) functionalized by 2-aminoethanethiol revealed that the STPM signal was independent of the underlying topography. Figure 2A shows the STM image surface structure of Au(111), with its characteristic pits and steps, similar to images obtained with longer chain alkanethiols.[12] Both STM and STPM images were acquired simultaneously.[23] The line scans in parts B and C of Figure 2 have been taken from cross sections of their corresponding images. The data in Figure 2B were taken from the cross section in Figure 2A (dashed line). The graphs show the STM signal (solid) and the corresponding STPM signal (dashed) at two temperature differences. The topography data clearly show height variations caused by pit formation and steps, whereas the ΔQ signal shows no response correlated with the topography. Even at a temperature difference of 20.3 °C we detected no ΔQ signal (Figure 2C). The root mean

(20) The solution was prepared by dissolving 5 mM 2-aminoethanethiol (Sigma) in methanol. The Au, after reacting with the solution for 5−10 h, was rinsed in H_2O and air-dried for the experiments.

(21) Allen, M. J.; Balooch, M.; Subbiah, S.; Trench, R. J.; Siekhaus, W.; Balhorn, R. *Scanning Microsc.* **1991**, *5*, 625−630.

(22) On occasion the drop diameter will not stabilize and snap but will contract in size until all of the solvent has evaporated. We have never found ordered monolayers from depositions of this kind.

(23) No molecular order of the 2-aminoethanethiol monolayer was detected. We used the Au(111) sample because the step size of the pits and steps (2.4 ± 0.2 Å) were similar to height variations on a molecular scale. We assume that the corrugation heights of monolayers were typically of the same order.

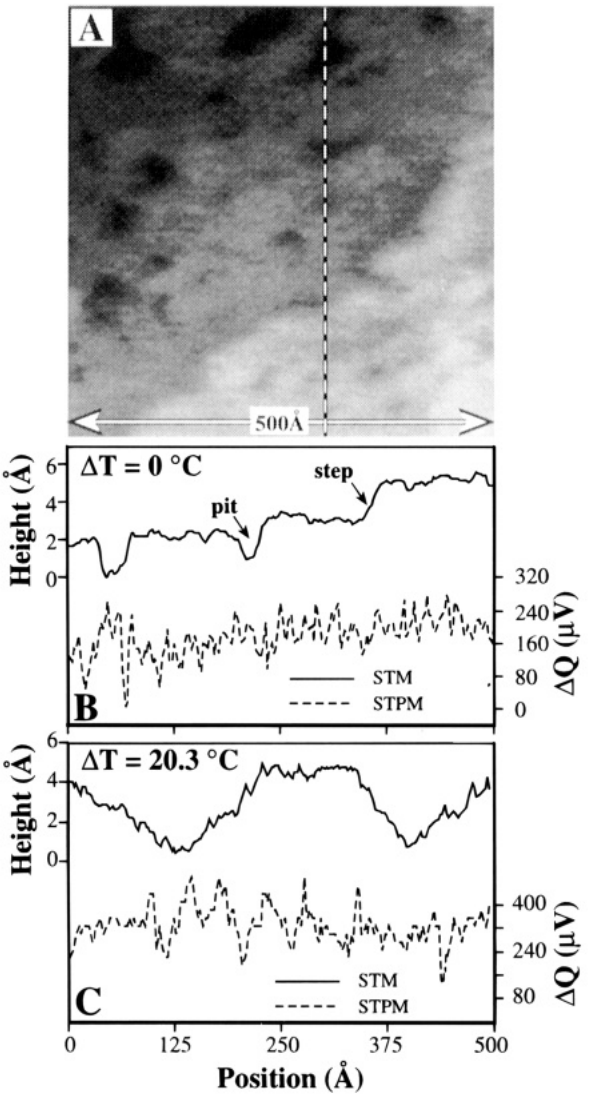

Figure 2. 2. Topographic independence of the STPM. Line scans through the STM data (A) are illustrated in part B. Monatomic steps and pits in the Au(111) are clearly resolved in the STM data (solid) and absent in the STPM data (dashed). At both room temperature (B) and $\Delta T = 20.3$ °C (C) there is no correlation of the topography in the STPM data. Gap impedance was 50 MΩ ($I_t = 400$ pA, $V_t = -20$ mV) and the sample was scanned at 1000 Å/s. Image size was 500 Å on a side.

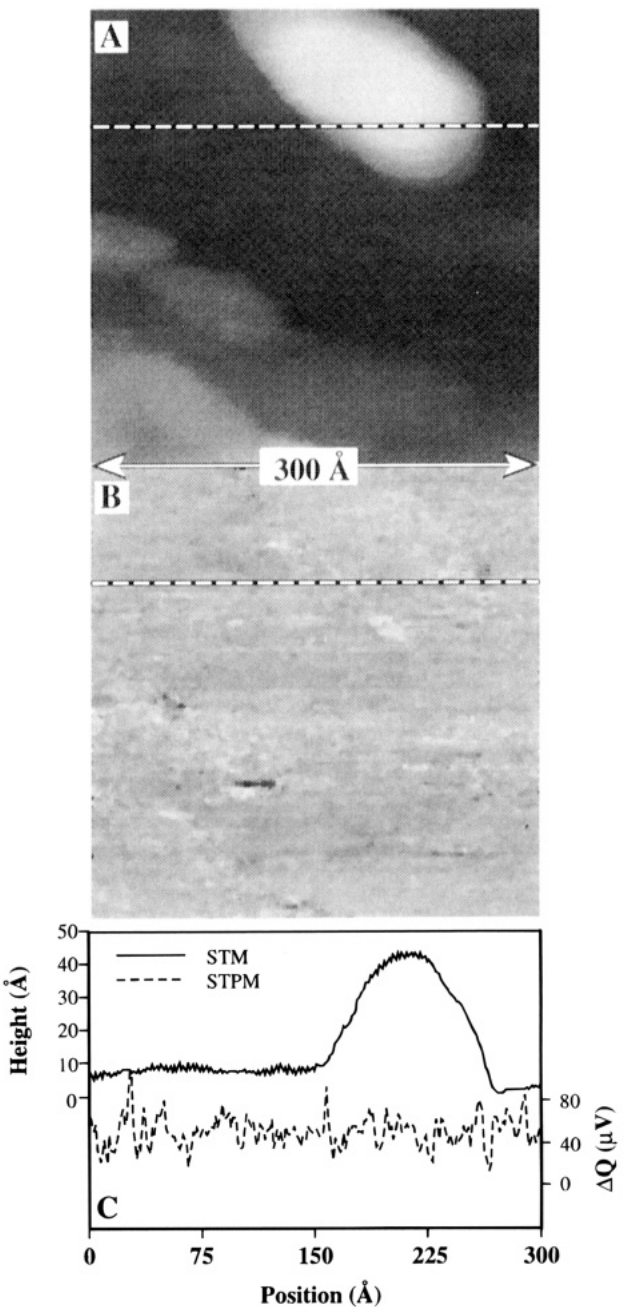

Figure 3. 3. Room temperature STM (A) and STPM (B) of a large grain on Au(111). Line scans of the data through the grain are displayed in part C. The STM signal (solid) measures the 44 Å high by 136 Å wide topography where the STPM signal (dashed) is independent of the topography. The gap impedance was 100 MΩ ($I_t = 100$ pA, $V_t = -10$ mV) and the sample was scanned at 2000 Å/s. Image size was 300 Å on a side. Because of topography errors due to the finite bandwidth of the STM amplifier, there is more noise in the STPM image (B) at the grain boundaries, where the topography changes abruptly.

square noise in these signals was about 70 μV (2.5 times higher than the noise on bare HOPG). This relatively high noise level results from noise in the STM current, typical for our measurements on Au. There is also more noise in the STPM signal when the topography changes abruptly, because of the limited bandwidth of our STM amplifier.

Figure 3A shows the STM image of a topographical feature of Au with a peak height of 45 Å. The image was scanned at a gap impedance of 100 MΩ. The corresponding STPM image is shown in Figure 3B ($\Delta T = 0$). There is no significant contrast in this image, and as with all our data on Au, the STPM signal was noisier in the region of the grain boundaries. In Figure 3C we show the STM and STPM data from a line scan across the image (dashed lines). For similar results on Au(111) at 200 MΩ (data not shown) there was also no ΔQ signal.

These results clearly show that the ΔQ signal acquired under feed-forward operation is topography independent as long as the gap impedance, or leakage currents, can be kept low enough. These data were acquired using imaging conditions typical for our guanine monolayer studies. Thus, we can safely conclude that the contrast we observe in the STPM images of the monolayers could not be a result of topographic variations or scanning inaccuracies.

Lateral Variations in Thermopower of Guanine monolayers. Figure 4 shows the STM (Figure 4A) and STPM (Figure 4B) images of a guanine monolayer on HOPG. These images were acquired simultaneously, as described above, at a gap impedance of 150 MΩ (1 nA at 0.15 V) and a scanner speed of 1000 Å/s. The substrate temperature was brought to equilibrium (~3 h) at $T_s = 71.8 \pm 1$ °C. There was a 26.5 °C temperature difference between the sample and the tip (i.e., the tip temperature, T_t, increased to 45.8 °C). The STM image exhibits rows of bright regions. The rows are separated by 16.8 Å. The distance between bright regions down each row is 6.9 Å

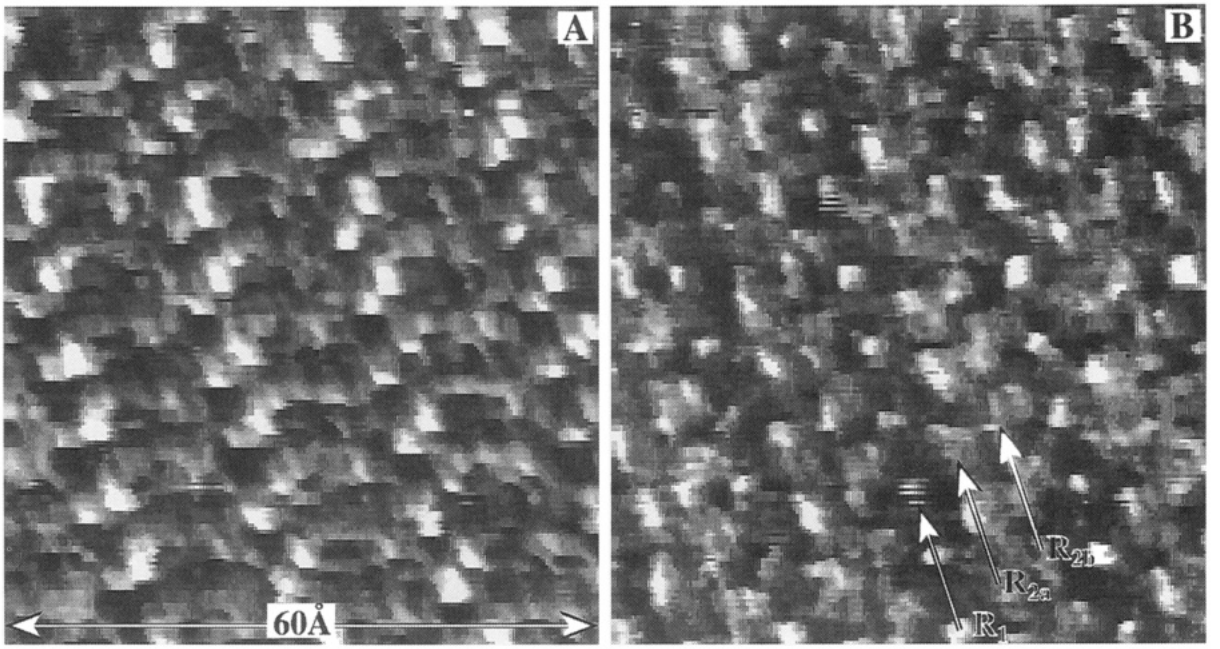

Figure 4. 4. STM (A) and STPM (B) images of a guanine monolayer adsorbed to HOPG. The substrate temperature was 71.8 ± 1 °C. There was a 26.5 °C temperature difference between the sample and the tip. The lattice vectors for the unit cell in both data are identical, where $a = 6.9$ Å, $b = 16.8$ Å, and $\alpha = 73°$. The STPM image is not a simple translation of the STM image. The gap impedance was 150 MΩ ($I_t = 1$ nA, $V_t = -150$ mV) and the sample was scanned at 1000 Å/s. Image size was 60 Å on a side. The lateral dimensions of the image were corrected to account for changes of the piezo-tube sensitivity (Å/V) with temperature.

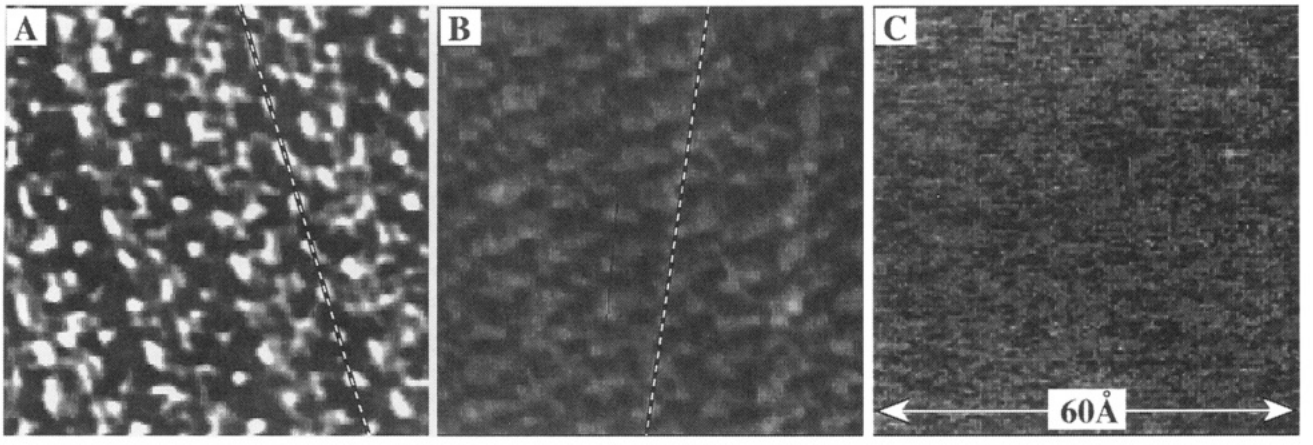

Figure 5. 5. Temperature dependence of the thermopower signal. All three STPM images are of the same guanine monolayer on HOPG. The corresponding STM images (data not shown) are similar to the STM image of Figure 4A. The contrast of the thermopower signal was measured from the peak to valley amplitude down the cross section of the data indicated by the dashed lines. The data in (A) were taken at the highest temperature difference, $\Delta T = 26.5$ °C and has the highest contrast, $\Delta Q = 504 \pm 73$ μV. At a lower temperature difference, $\Delta T = 18.5$ °C (B), the contrast is correspondingly lower, $\Delta Q = 94 \pm 24$ μV. At room temperature with $\Delta T = 0$ °C (C), there is no contrast in the STPM data, only noise, $\Delta Q_{RMS} = 58$ μV. The gap impedance for all three images was 150 MΩ ($I_t = 1$ nA, $V_t = -150$ mV) and the samples were scanned at 1000 Å/s. Image size was 60 Å on a side.

with an angle of $\alpha = 73°$ separating these two lattice vectors. Each bright region in the row is elongated, with a major axis of 6.1 ± 0.4 Å and a minor axis of 3.0 ± 0.2 Å. Between the rows there is some contrast, albeit lower than that down the row. The contrast down the valley also consists of a row of bright regions, but lower in amplitude.

Figure 4B is the STPM image of the previously described guanine monolayer. This is the first measurement of lateral variations of thermopower on an organic molecule. The image is also periodic. The lattice of the STPM image is described by the same unit vectors characteristic of the STM image (Figure 4A). However, and importantly, the information in the STPM image is not a simple translation of the STM image. The STPM image consists of rows of localized bright regions (indicated by R_1 in Figure 4B) translated by 2.4 Å in a direction 82° from the lattice vector defining the STM rows. Between the rows of bright spots there are two rows of more elongated but still localized high contrast (indicated by R_{2a} and R_{2b} in Figure 4B). The corrugation amplitude down the brightest row is 504 ± 73 μV, and for the other rows, 415 ± 41 μV.

These images were reproducible, and the lattices were stable even at low gap impedance. Figure 4B shows the highest contrast and best lateral resolution STPM image that we acquired. Typically, the STM image was of good contrast, but the STPM image was degraded (about half the contrast). We have not yet determined if the loss of contrast and lateral resolution was due to the quality of the monolayer, the quality of the tip, or a combination of both.

The Guanine Lattice: Temperature Dependence of the Thermopower Image. In Figure 5 we show three STPM images of guanine thermally deposited on HOPG which illustrate the temperature dependence of the thermopower signal. All three images are from on the same sample. The STM images of all three (data not

shown) reveal typical ordered monolayers of guanine.[24] The tunneling gap impedance for these images was 150 MΩ. The high temperature data were acquired first, followed by successively lower temperatures. The contrast in parts A and B of Figure 5 measured down structurally identical rows (indicated by the dotted lines) is defined by the peak to valley amplitude of the thermopower. The lateral variations of the thermopower signal decrease with decreasing ΔT where $\Delta Q = 504 \pm 73\ \mu$V for $\Delta T = 26.5$ °C, $\Delta Q = 94 \pm 24\ \mu$V at $\Delta T = 18.5$ °C, and the STPM noise was $\Delta Q_{RMS} = 58\ \mu$V at $\Delta T = 0$ °C. The thermopower sensitivity Σ was thus 49 μV/°C.[25] The temperature dependence on the signal clearly indicates that these were not electrostatic or localized charge measurements.

The Guanine Lattice: Interpretation of the STM Images. In Figure 6 we show a typical room temperature STM image of a thermally deposited self-assembled monolayer of guanine on HOPG. These data were acquired with a gap impedance of 2.5 GΩ (0.2 nA at 0.5 V) at room temperature. By use of an AFM, large areas (~1 μm^2) of the HOPG substrate were surveyed. The guanine cover approximately 10−50% of the HOPG surface, distributed in irregular patches 200−700 Å wide. The patches consist of multilayers (two to three layers) with ~5 Å step heights (data not shown). However, these multilayers were never seen with the STM. The interlayer stacking distance of these types of conjugated ring systems is 3.4 Å.[26] Although we can see atomic resolution with the AFM tip over the clean HOPG, we do not observe any structure in the multilayers, indicating that they are not strongly bound to each other and possibly disordered. However, the STM does image the guanine monolayer close to the HOPG surface, leading us to believe that the tip pushes through the loosely bound upper layers, imaging only those more strongly coupled to the underlying HOPG.

The STM images of the monolayers consist of periodic rows of bright regions, separated by valleys. There is a bimodal distribution of the lattice size with periods of 16 ± 0.5 and 21 ± 0.5 Å. Down each row there is also periodic structure. At room temperatures, the images exhibit a 9.6 ± 0.5 Å period down the row. These structures correlate reasonably well with other experimental studies (10.5 Å × 19.4 Å Heckl *et al.*[10] and 9.0 Å × 17.0 Å Srinivasan *et al.*[27]).

There were other structures observed on rare but reproducible occasions. Least often, we observed more symmetric lattices where the valleys also contained equally bright regions. More commonly, the images were disordered and noisy. Sometimes we observe lattice structures similar to those in Figure 6; however the periodicity down the row was smaller, typically 7.5 ± 0.2 Å. Images of ordered and stable monolayers of guanine 200 Å by 200 Å in extent were observed. However, for any given deposition, atomic resolution HOPG was imaged most (>50%) of the time. Given the many different hydrogen bonding schemes for the guanine system, we are not surprised to see variations in the lattice size and structure. We have similar evidence of variability for the adenine system.[28]

Images of these monolayers were typically acquired at elevated substrate temperatures (*viz.*, 55−72 °C). The samples were held at these temperatures for several hours before measurements were made. These heated lattices always exhibit shorter periodicity down the rows, with a period typically 7.5 ± 0.5 Å, but as large as 8.5 Å and as small as 6 Å (we have corrected for temperature variations in the piezo-tube sensitivity). We believe that the deposited monolayers were incorporated with water to form a possibly cross-linked network of hydrogen bonded molecules. Upon heating, the 2D lattice slowly dehydrates and evolves to a new and smaller minimum energy configuration. Even as the temperature of the sample was reduced (and also at room temperature), only the smaller guanine lattices were observed. Further studies are in progress, but the fact that we never observe the large 10 Å structure after heating supports our dehydration hypothesis.

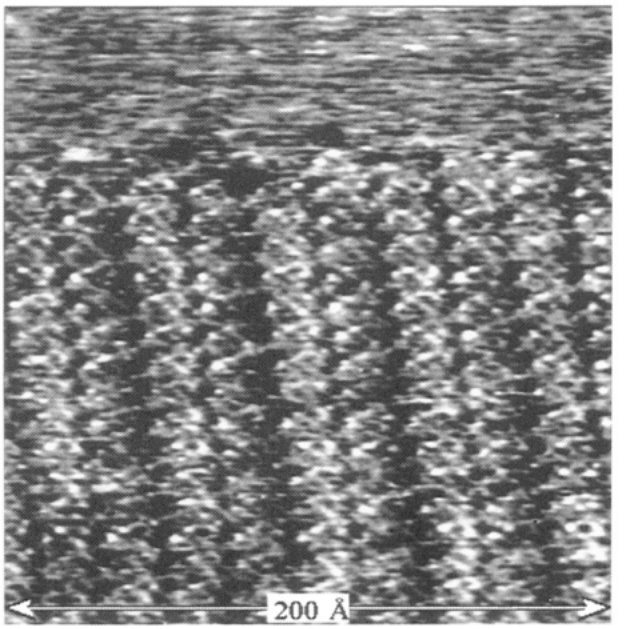

Figure 6. 6. Typical room temperature STM image of guanine adsorbed to HOPG. The sample had not been heated. The upper portion of the image is characteristic of a low density disordered layer of guanine. The ordered monolayer in the lower $^4/_5$ of the image has lattice vectors: $a = 9.6 \pm 0.5$ Å, $b = 21.0 \pm 0.5$ Å and $\alpha = 88°$. The gap impedance was 2.5 GΩ (I_t = 200 pA, V_t = −500 mV) and the sample was scanned at 4000 Å/s. Image size was 200 Å on a side.

We associate the bright regions in the STM image with guanine molecules. These heat-treated samples may be compared to the room temperature images of guanine by Heckl *et al.*[10] and adenine by Allen *et al.*[21] Both interpret their images to consist of bimolecular rows separated by water via hydrogen bonding. Srinivasan *et al.*[27] also used STM to image electrochemically condensed guanine monolayers on HOPG. They propose a model where the rows are monomolecular, and the valley contains two additional planer guanine molecules. It is interesting that the molecules in the valleys do not show up in their topography image. In the theoretical analysis of adenine on HOPG by Ou-Yang,[29] the overall brightness of the molecule depends on its registration with the graphite lattice.[30] It is therefore plausible that the spots in the valleys of the STM images reported here also correspond to guanine. The convoluted nature of these images make molecular identification difficult and the need for additional information essential.

The Guanine Lattice: Interpretation of the STPM Images. Support for our interpretation of the ther-

(24) None of the images were filtered, but the contrast has been adjusted in order to illustrate the actual signal contrast in the measured data.

(25) The data in Figure 5A are some of our best, more typical data at about the same ΔT has a lower contrast of ~240 μV, yielding $\Sigma = 18.7$ μV/°C. The lower thermopower contrast corresponds with poorer lateral resolution in both the STM and STPM.

(26) Voet, D.; Rich, A. In *Progress in Nucleic Acid Research and Molecular Biology*; Davidson, J. N., Cohn, W. E., Ed.; Academic Press: New York, 1970; Vol. 10; p 202.

(27) Srinivasan, R.; Murphy, J. C.; Fainchtein, R.; Pattabiraman, N. *J. Electroanal. Chem.* **1991**, *312*, 293−300.

(28) Poler, J. C.; Cox, E. C. To be submitted to *JVST B.*

(29) Ou-Yang, H.; Marcus, R. A.; Källebring, B. *J. Chem. Phys.* **1994**, *100*, 7814−7824.

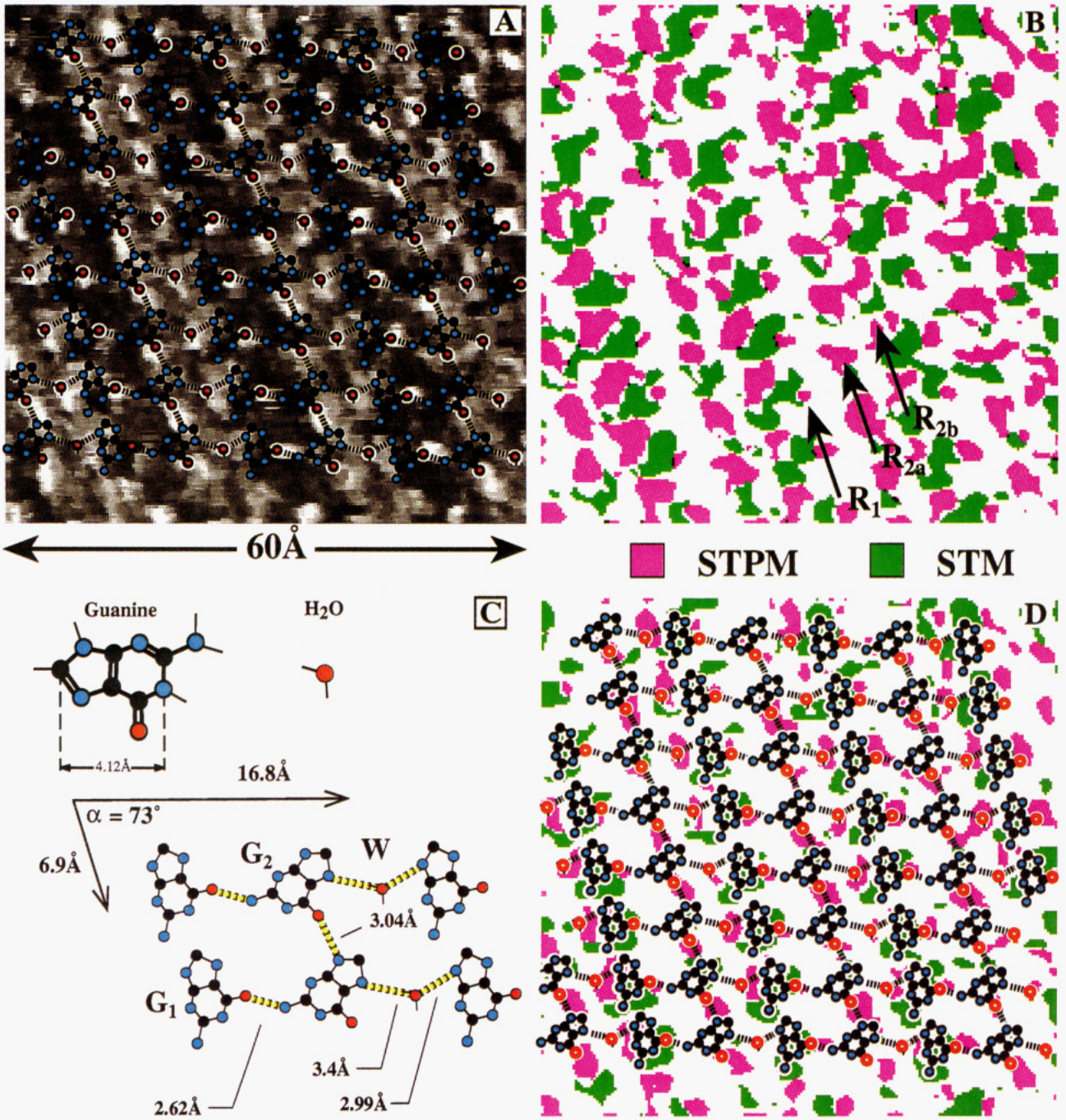

Figure 7. 7. Interpretation of STPM images. STPM data of Figure 4B are shown with a proposed model of the guanine lattice superimposed (A). A false color representation of both the STM and STPM (green and pink, respectively) images (B) illustrate the unique information contained in the two representations of the monolayer. The unit cell in our model (C) consists of one H_2O and two guanine molecules. The unit cell is duplicated and translated by the lattice vectors from the data and superimposed on the merged STM and STPM image (D). Every bright region in the STPM data (pink) is associated with an O atom in the model (also evident in Figure 7A). Every bright region in the STM data (green) is associated with a guanine molecule.

mopower images described above rests on the following: the dependence of chemical potential on electronegativity; the local density of states calculations; and the ability to use our interpretation to build a plausible model of the guanine lattice.

In our preliminary interpretation of the STPM signal we associated bright regions in the STPM image with regions of high electronegativity. From the analysis of Williams and Wichramasinghe,[18] the thermopower signal is related to the thermal gradient of the local chemical potential ($\partial\mu/\partial T$). At constant ΔT, spatial variations in thermopower result from variations in μ. Theoretical analysis by Parr and Yang[31] relate chemical potential to electronegativity [$\mu \sim -(I + A)/2$]. The high electronegativity of O in the guanine molecule could yield the high ΔQ in the STPM images.

On the basis of Støvneng and Lipavsky's analysis,[32] one should be able to calculate $\Delta Q(x,y)$ for the various chemical moieties on the surface. They derive that ΔQ is propor-

(30) We were sometimes fortunate and obtained images with well-resolved monolayers and images of the underlying graphite. From these data we conclude that the monolayer was not arranged in a commensurate epitaxy with the substrate. From our best results (data not shown) we can measure the angle between the guanine rows and the underlay lattice to be rotated by 25° from the [100] direction. Other data exhibit a 13° rotation. We observed differing STM image contrast in the guanine monolayers with small variations (only 8°) of the lattice to substrate orientation.

(31) Parr, R. G.; Yang, W. *Density functional theory of atoms and molecules*; University Press: Oxford, 1989; Vol. 16, p 74.

(32) Støvneng, J. A.; Lipavsky, P. *Phys. Rev. B* **1990**, *42*, 9214–6.

tional to the logarithmic derivative of the LDOS. They calculated ΔQ for Mo and S based on Lang's[33] calculation of the LDOS (ϱ) for these atoms on a jellium substrate. We have a preliminary estimate of ΔQ for C and O based on LDOS calculations by Lang,[34] similar to those stated above on a metal (jellium model with $r_s = 2$). We calculated ΔQ from the slope, $(\partial\varrho/\partial E)/\varrho$, of his data, evaluated at $E = E_F$. The lateral variation in thermopower for O on a jellium was 20% larger than for C on the same substrate. Although this system is oversimplified to explain an organic molecule on a real substrate, it supports our hypothesis that the higher ΔQ in our images is associated with the O atom. On the basis of this hypothesis, we have built a model of the guanine lattice.

The guanine monolayer lattice is illustrated in Figure 7. Figure 7A shows the STPM data shown in Figure 4B with our proposed lattice superimposed. The data in Figure 7B are given a false color representation of both the STM and STPM images. The data from each image were binarized, assigned a color, and merged. The STM and STPM data are green and pink, respectively. From this representation, it is clear that the two images give unique information about the molecular species in the monolayer. Previous results comparing STM to STPM[18] exhibited a simple translation of a high symmetry lattice (e.g., the hexagonal lattices of HOPG and MoS_2), which does not provide additional information about the sample. The monolayers we have studied exhibit a more complex unit cell. Because the structure of the unit cell in the STPM image is so different from that of the STM image, we can use this technique to obtain additional information about the sample (e.g., molecular orientation within the unit cell, and possibly, inclination of the molecule to the underlying substrate).

The unit cell used to build our proposed model is illustrated in Figure 7C. The same model of the guanine lattice (Figure 7A) is also superimposed on the image in Figure 7B and illustrated in Figure 7D. The unit cell consists of one H_2O and two guanine molecules. To build this model, we first assumed that the guanine O atoms correlate with the localized bright regions down row R_1 in the STPM image (Figure 7A). The molecule was then oriented about the O atom to maximize its overlap with the bright regions in the STM image (green). This molecule is labeled G_1 in Figure 7C. There are two more bright regions in the unit cell of the STPM image. A second guanine (G_2, Figure 7C) was placed so its O atom coincided with a bright region down the row labeled R_{2a} (Figure 7A) of the STPM image. There was not enough room to add a third guanine molecule to the unit cell. A water molecule (W, Figure 7C) was placed at the position of the corresponding bright region on the row labeled R_{2b} (Figure 7A). The stability of the guanine monolayers to tip-induced disordering suggested that there is significant cross-linking of the hydrogen bonding network. Therefore, G_2 and W were rotated about their O atoms to maximize hydrogen bonding in the lattice. Finally, each guanine molecule is hydrogen bonded to another, and to one H_2O. Each G_2 molecule is hydrogen bonded to two other G_2 molecules in the unit cell above and below, resulting in a cross-linked hydrogen bonding network.

In this model, every bright region in the STPM signal is associated with an O atom. The high contrast regions down the rows in the STM images (green) are associated with a molecule, as are the lower contrast regions in the valleys. The hydrogen bonding scheme uses accepted bond lengths and angles.[35] From STM data alone, we would have very little confidence in the proposed model.

(33) Lang, N. D. *Phys. Rev. Lett.* **1987**, *58*, 45–48.
(34) Lang, N. D. Personal communication.

Conclusions

We have developed a novel scanning thermopower microscope. We have confirmed and extended previous experimental results establishing an ability to measure local variations of thermopower at atomic resolution. We have provided experimental evidence to support theoretical analysis of the temperature dependence of thermopower variations. This study is the first report of atomic scale resolution thermopower images of an organic molecule.

Because of the weak distance dependence of the thermopower signal, and the feed-forward nature of our data acquisition method, the STPM images were insensitive to sample topography. This enables an imaging technique that is not convoluted with substrate roughness, disorder, or defects. This technique also enables the imaging of single molecules regardless of their orientation on the substrate (i.e., nonplanar).

We have proposed that the contrast in the STPM images is associated with the O moieties in the guanine monolayer lattice. Electronegativity arguments and preliminary density of states calculations support this hypothesis. A plausible model of the guanine lattice correlates the O atoms with the bright regions in the thermopower image.

Many STM images of organic or biological molecules cannot resolve internal structure, orientation, or identity of the species. The additional information provided by the STPM images helps deconvolute this information. We are currently investigating other monolayers were the constituents contain more that one O atom. This will further limit the possible orientations of the molecules. However, more accurate theoretical analysis is required to develop this technique into a viable spectroscopy. Local density of states calculations for organic molecules on real surfaces like HOPG and Au(111) are necessary.

We found (data not shown) that ΔQ is proportional to the temperature difference between the tip and sample, with a slope of $\Sigma = 10.2\ \mu V/°C$[36] for bare HOPG. The relative sensitivity, Σ, for thermopower measurements of guanine monolayers adsorbed to HOPG is 2–3 times larger than for the bare substrate. This result is consistent with the observation that Σ for the semiconductor MoS_2 is much larger than it is for the semimetal HOPG[37] (i.e., a larger bandgap) since ΔQ depends on the energy distribution of the density of states. The energy separation between the highest occupied molecular orbital (HOMO) and lowest unoccupied molecular orbital (LUMO) of the guanine molecule is analogous to the band gap in a semiconductor. It then follows that a measurement of ΔQ versus temperature for molecules with differing HOMO–LUMO gaps should yield a different value of Σ. We hold the temperature constant, therefore variations in ΔQ are a measure of the local Σ of our sample and thereby identify the molecular species. We believe this method holds promise toward the development of a single molecule spectroscopy.

Acknowledgment. This work was supported by grants from the NSF and NIH. We acknowledge the generous support of the Princeton Materials Institute in providing access to a scanning tunneling microscope and the help of D. Peoples. Many interesting discussions with J. A. Støvneng and LDOS calculations provided by N. D. Lang are appreciated.

LA940946K

(35) Pauling, L. *The Nature of the Chemical Bond*, 3 ed.; Cornell University Press: Ithica, NY, 1980, p 453.
(36) The absolute accuracy of this sensitivity may be underestimated due to difficulties in measuring the actual temperatures of the tip and substrate at the tunneling junction.
(37) Williams, C. C.; Wichramasinghe, H. K. *J. Vac. Sci. Technol. B* **1991**, *9*, 537–539.